

ISTITUTO NAZIONALE DI FISICA NUCLEARE

zione di Milano

INFN/AE-77/13
2 Novembre 1977

P. G. Rancoita: COHERENT AND MULTIPARTICLE
PRODUCTION ON NUCLEI IN FRAMM EXPERIMENT.

P. G. Rancoita^(*): COHERENT AND MULTIPARTICLE PRODUCTION ON NUCLEI IN FRAMM EXPERIMENT.

(Talk given at Highly Specialized Seminars on Multiparticle Production, Erice, 23 Maggio-5 Giugno, 1977).

1. - INTRODUCTION AND PHYSICAL MOTIVATIONS.

Since few years it has been emphasized that the nuclear phenomenon permits to understand something more of the hidden dynamics which cannot immediately be seen in h-h collisions^(1, 9).

In this sense the nucleus is a very dense detector. The time scale, over which the internal processes developed, is very long compared to usual time scale of the hadronic interaction or formation.

In principle the internal dynamics may be considered as the clue which allows to set together A nucleons (where A is the atomic number) and does not generate any difference between bound and free nucleons.

Suppose τ is the characteristics collision time in h-h c. m. system; in lab. frame it is Lorentz dilatated in such a way that, in high energy collisions, the hadronic system formed in the primary collision may interact again before reaching its own asymptotic state.

One may therefore think that the nuclear interactions offer the unique possibility of studying the space-time development of hadronic processes.

Let us try to give a glimpse inside the experimental situation for both coherent and incoherent production.

The Glauber Theory has been proposed for elastic scattering on nuclei^(10, 11) and then modified for diffraction dissociation by Kölbig and Margolis⁽¹²⁾.

Looking to coherent production, see Fig.1, the standard Glauber Theory may be summarized in five points:

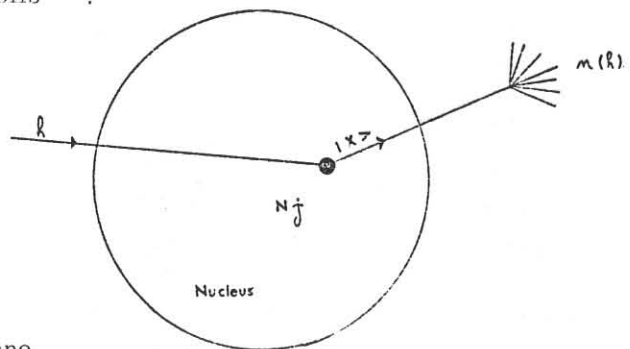


FIG. 1

(*) and Istituto di Fisica dell'Università di Milano.

- a) elastic scattering of the hadron h before the production point
- b) instantaneous production of a hadronic system $|X\rangle$ in its asymptotic state
- c) only one production point on the nucleon N_j
- d) elastic scattering of the produced system $|X\rangle$ after the production
- e) the only unknown quantities in the theory are σ_2 and a_2 which are respectively the total cross-section and the ratio of real to imaginary part of the scattering amplitude of the system $|X\rangle$.

Generally there is a good agreement between theory and experimental data for what concerns the differential cross-section; the unclear point is the dip filling in the first minimum region.

The total cross section of the instable system $|X\rangle$ has been determined in many experiment, covering few exclusive channels and large mass regions^(13, 18). The data may be summarized as follow:

- a) σ_2 is lower or $\sim \sigma_{inc}$
- b) σ_2 decreases with the number of particles in final state
- c) σ_2 decreases with increasing mass of $|X\rangle$

In Table I a resume of the present data on σ_2 derived for different channels of coherent dis-

Inc. energy (GeV)	produced mass (GeV/c ²)	Energy (GeV)						
		1.0	1.2	1.4	1.6	1.8	2.0	2.2
$K^+A \rightarrow K^+\pi^+\pi^-A$			22*		22*	14*		$\Sigma \approx 2.0 - 2.5$
$\pi^-A \rightarrow \pi^+\pi^-\pi^-A$								
8.9		29*	23*					* $\Sigma \approx \pm 1.5 - 2.$
15.1		23*	19*	16.*	20.**			** $\Sigma \approx \pm 3.5$
22.5		27.						
$\pi^-A \rightarrow \pi^+\pi^-\pi^-A$ 0 ⁻ state								
8.9		60. ± 20.						
15.1		49. ± 8.						
22.5		53. ± 11.	27.5 ± 2.					
$\pi^-A \rightarrow \pi^+\pi^-\pi^-A$ 1 ⁺ state								
15.1		17.*						* $\Sigma \approx \pm 1.0$
22.5		23.4*	22.0*					
$nA \rightarrow p\pi^+\pi^-A$								
22.5			36.*	28.*	24.*	21.*	17.*	* $\Sigma \approx \pm 1. mb$
$pA \rightarrow p\pi^0A$ $nA \rightarrow p\pi^-A$								** $\Sigma \approx \pm 2. mb$
22.5			33. ± 7.					
6. - 16.			36. ± 7.					
100. - 300.			39.					

TABLE I

sociation is given; in Table II the σ_2 's for 5π dissociation at 15 GeV are listed.

A PWA has been also performed on the 3π coherent production at 9, 15 and 23 GeV⁽¹⁹⁻²⁶⁾.

The data show that:

- a) only 1^+ and 0^- waves are present in the A_1 region
- b) in A_1 region $\sigma_2(1^+)$ is lower than the single particle cross-section and $\sigma_2(0^-)$ is more or less twice $\sigma_2(1^+)$
- c) $\sigma_2(0^-)$ again has a low value after the A_1 region.

Many modifications have been proposed to the standard Glauber Theory⁽²⁷⁻³⁴⁾, in order to explain the transparency of nuclear matter, the behaviour of 0^- and 1^+ waves total cross section and the dip filling.

The common connection between the models is that neither an asymptotic final state $|X\rangle$, nor only an elastic scattering of $|X\rangle$ in the nucleus are required.

Another experiment on coherent diffraction dissociation has been carried out at 40 GeV⁽³⁵⁾ and the first data will be available by the end of 1978.

Since many years ago, cosmic ray physicists concluded that multiplicity produced is weakly dependent from the atomic number A.

At present the data on multiple production on nuclei come from cosmic ray measurements, e-mulsion exposures at accelerators^(36, 37) and one counter experiment at FNAL^(4, 8, 38, 39). It is convenient to look the data in terms of few parameters, namely: $R_A, \bar{\nu}, N_h$

$$R_A = \frac{\langle n \rangle_A}{\langle n \rangle_P}$$

where $\langle n \rangle_A$ is the average number of charged relativistic particles ($\beta \geq 0.7$) produced in inelastic collisions with a nucleus A; $\langle n \rangle_P$ is the average number of charged relativistic particles produced with a proton.

$$\bar{\nu} = \frac{A \sigma_{hP}(\text{inelastic})}{\sigma_{hA}(\text{inelastic})}, \quad N_h = N_g + N_b$$

where N_g is the number of grey tracks ($0.3 < \beta < 0.7$) and is practically the number of protons coming from quasi direct interaction. N_b is the number of black tracks ($\beta < 0.3$) and may be considered the number of protons with an energy inside the evaporation spectrum.

The energy dependence of R_A is derived for emulsions. The data are consistent with R_{em} independent from energy when $E > 60$ GeV.

It is well established that R_A increases very slowly with A, is more or less linear dependent from $\bar{\nu}$ and lower than 2.5 for very heavy nuclei, see Fig. 2 (from ref. (38)).

At small angles (which means projectile fragmentation region in pseudorapidity plot) no difference appears between nucleon and nucleus, as otherwise seen in bigger angle regions, see Fig. 3 (from ref. (38)).

A linear dependence of $\langle n \rangle_s$ (which is the average number of fast secondaries produced at fixed N_h , in emulsion) from N_h may be affirmed.

A great deal of theoretical work has been developed on multiparticle production on nuclei (see

TABLE II - Results of optical model fits to σ_{coh} for $\sigma_2(5\pi)$ (mb) and C_0 (arbitrary units).

Mass interval (GeV)	Parameters		
	$c_0 = 0$ c_2	$c_0 = 1.12 f$ $\Delta \sigma_i$ stat.	$\alpha = 0.545 f$ $\Delta \sigma_i$ system.
1.5-19	17	5	+ 8 - 7
1.5-17	10	7	+ 8 - 4
1.7-19	13	10	+ 9 - 6

FIG. 2

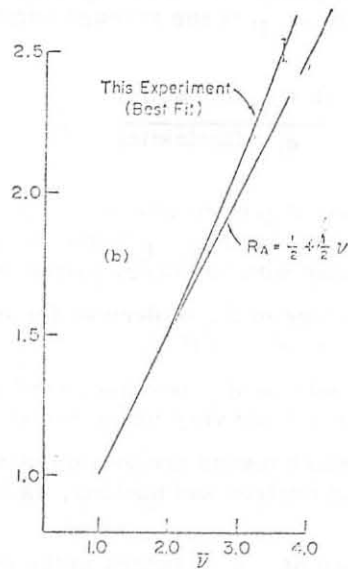
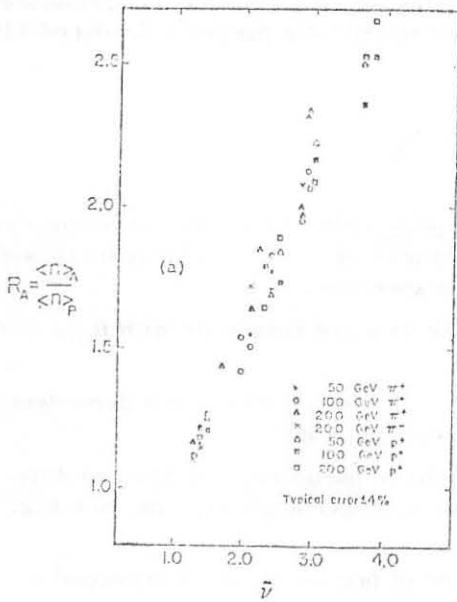
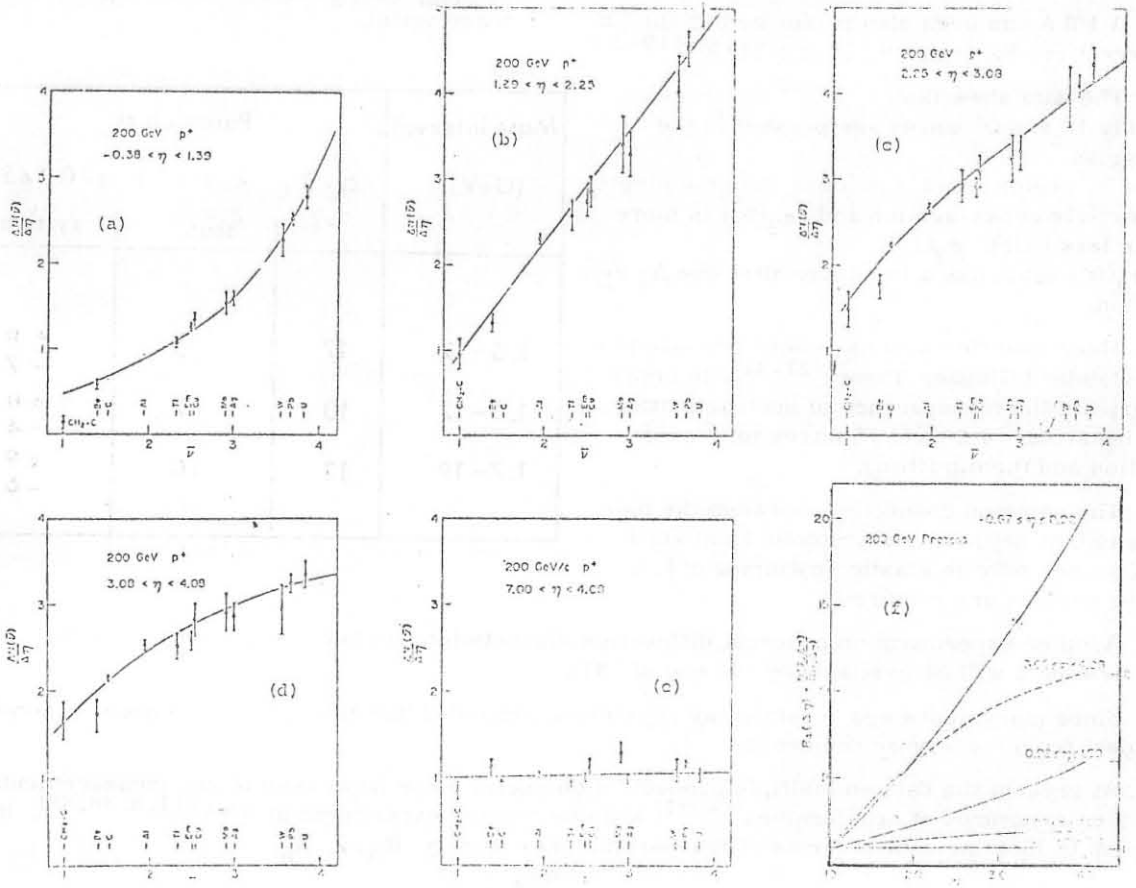


FIG. 3

ref. (8) and references therein).

But it is still impossible to choose among models with the present experimental situation.

Several refined measurements are needed; firstly it is necessary to get a rapidity distribution instead of the pseudorapidity one, secondly an analysis of the type and the energy of nucleons coming from the struck nucleus⁽⁴⁰⁾.

As general remark, we can say that the striking features of coherent and incoherent production on nuclei are:

- a) the total cross-section of the produced system is nearly the same of the incident particle;
- b) the multiplicity produced on nuclei excludes any cascading model inside the nucleus and is concentrated in the target fragmentation region.

These experimental data agree with the idea that the interaction on nuclei are a powerful tool for understanding the space-time development of hadronic system.

Moreover, the coherent interaction supplies a simple and direct way for selecting either spin-parity series in diffractive production or diffractive Coulomb dissociation.

In the latter case the production cross-section goes as Z^2 and is increasing with the energy.

As consequence processes such as coherent production of $D \bar{D}$ and Coulomb production of η_c ($2.8 \text{ GeV}/c^2$) may be selected when the photon is coherently diffracted on a target nucleus.

2. - FRAMM EXPERIMENTAL SET UP AND NUCLEAR TARGETS.

FRAMM experiment is expected to start its data taking in June 1978, at CERN-SPS.

It is an Italian Collaboration of Sezioni INFN ed Università di Milano Pisa e Roma and Laboratori Nazionali di Frascati^(41, 42, 43).

It will work with P , \bar{P} , K^+ , π^+ beams in the energy region $100-400 \text{ GeV}$ and a photon beam with top energy of 200 GeV .

The apparatus consists of: a forward spectrometer, a vertex detector and sensitive nuclear targets.

2.1. - Forward Spectrometer.

The spectrometer comprises four magnets.

The first one has a gap of 50 cm , 1 m long and a maximum bending power of 1.3 Tm .

The distance from the target is 1.5 m and the acceptance angle of $\pm 90 \text{ mrad}$, which corresponds to 90° in c. m. system for a particle of an average P_T at $300 \text{ GeV}/c$.

The subsequent magnets are standard PS beam transport magnets⁽⁴¹⁾.

Five sets of drift chambers are positioned as shown in Fig.4, each set consists

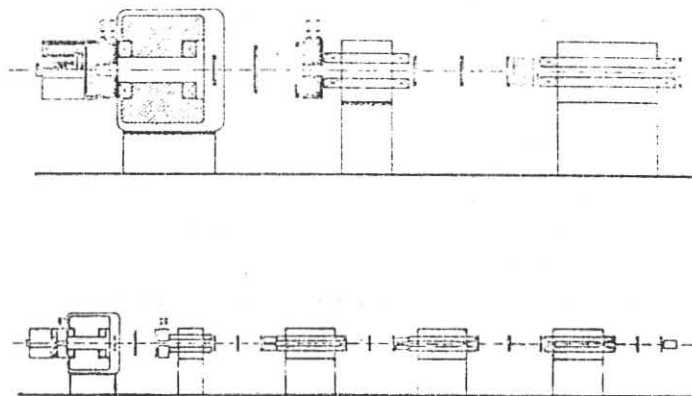


FIG. 4 - General layout of FRAMM experiment. The sketch presented below is a general top view of the forward spectrometer with vertex detector. In the drawing presented above, only first three magnets with drift chambers and photon detectors are shown in detail.

of three chambers, each of them has two orthogonal planes with a sense wire spacing 4.8 cm. The obtained resolution on the drift coordinate is $\Delta X = \pm 0.14$ mm, while the resolution of the delay line, flanking each sense wire, is $\Delta Y = \pm 2$ mm.

The calculated resolution is $\Delta P/P \approx \pm 0.5\%$ for produced particles inside the acceptance cone of the spectrometer.

The first two photon detectors (see Fig. 4) are scintillation counterlead sandwiches, which cover photons produced in the angular ranges $7^\circ \leq \vartheta \leq 30^\circ$ and $1.7^\circ \leq \vartheta \leq 7^\circ$ respectively.

They have an energy resolution of 9% and a space resolution of ± 2 mm.

The other ones are lead-glass Čerenkov counter matrices, covering the angular region of $0^\circ \leq \vartheta \leq 1.7^\circ$. The expected energy and space resolution is 4.5% and ± 2.5 mm respectively.

The π , K, P distinction, up to 40 GeV, is made possible by two Čerenkov counters positioned inside the 1st and 2nd magnet.

2.2. - Vertex Detector.

Surrounding the sensitive nuclear target is placed the vertex detector, see Fig. 5.

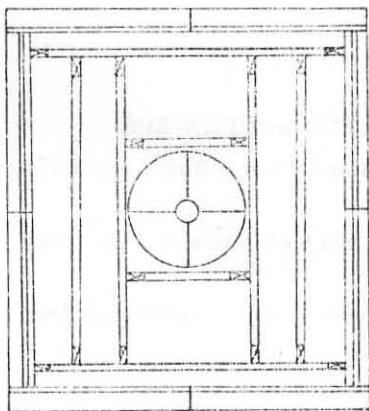


FIG. 5- Front view of FRAMM Vertex detector with inserted η_c target.

It consists of a box of four drift chambers which allow a resolution on the polar angles of $\Delta\vartheta \approx 3$ mrad.

Immediately after a box of scintillation counter are positioned. They perform the identification and the measurement of the kinetic energy of photons between T=30 and T=600 MeV.

Finally four lead-scintillation counters are used for detecting photons outside the region covered by the forward spectrometer.

Downstream from the nuclear sensitive target a set of three drift chambers measures the direction of particles between few degrees and 45° .

They are followed by two MWPC's for fast tracks counting and trigger purposes.

2.3. - Sensitive Nuclear Targets.

These targets are thought to be placed inside the vertex detector; three of them are listed below following the time scheduled for FRAMM experiment.

The Milano group is also improving the silicon live-target already used in other two experiments.

2.3.1. - η_c target.

This target provides a fast trigger to FRAMM spectrometer when data are taken on coherent photoproduction.

The detector is a cylindrical plastic scintillator, shown in Fig. 6, subdivided in four sectors, each of them seen by two photomultipliers RCA 8575, working in coincidence.

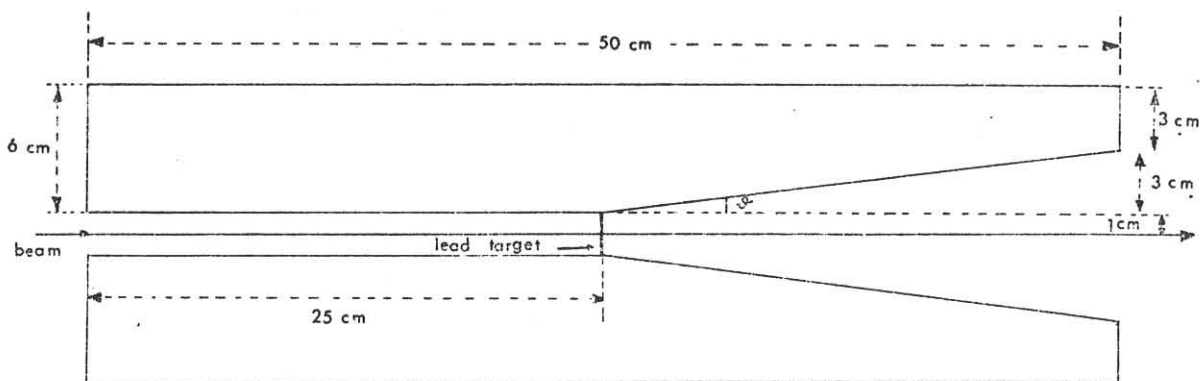


FIG. 6

How these sectors have to work together will be decided after the first tests on the 200 GeV photon beam.

600 μm of lead are placed in the center of the scintillator, whose forward cone is ± 90 mrad.

The secondaries produced in a coherent reaction are expected to be inside this cone.

In general FRAMM forward spectrometer seems to be ideal for coherent photon or hadroproduction on nuclei, because:

- a) there is a simultaneous detection of charged particles and photons. The detection efficiency is nearly independent from the multiplicity of final state⁽⁴²⁾.
- b) It is possible to reconstruct the coherent produced mass with a resolution of ≈ 100 MeV (FWHM)⁽⁴³⁾.

What we ask to the detector is a fast anticoincidence signal for incoherent event.

With a photon beam it is possible to study both pseudoscalar and vector meson photoproductions.

The former are produced via Primakoff effect, see Fig. 7, in which a virtual photon is exchanged and represents the inverse process of the PS meson decay in $\gamma\gamma$.

The differential cross section is:

$$\frac{d\sigma}{d\Omega} = 8a \Gamma_{\gamma\gamma} \frac{Z^2 \beta^2 E^4}{m^3} \frac{F^2(q)}{q^4} \sin^2 \vartheta$$

where:

$a = 1/137$

$\Gamma_{\gamma\gamma}$ is the two photon decay

m is the photoproduced mass

β, E are the velocity and the energy of the particle

ϑ is the production angle

q is the momentum transfer

$F(q)$ is the electromagnetic form-factor of the nucleus

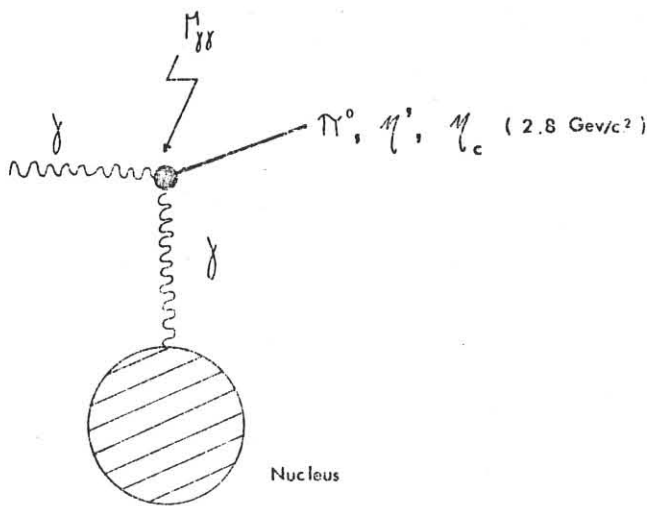


FIG. 7

In this formula the only unknown quantity is $\Gamma_{\gamma\gamma}$. With the FRAMM it is possible to measure both integrated cross section and the branching ratio toward $\gamma\gamma$ decay.

In such a way a direct measurement of the lifetime of PS mesons may be performed, in particular the η_c ($2.8 \text{ GeV}/c^2$).

In Fig. 8 (from ref. 43) the mass acceptance of the apparatus is shown for $\pi^0, \eta, \eta', \eta_c$.

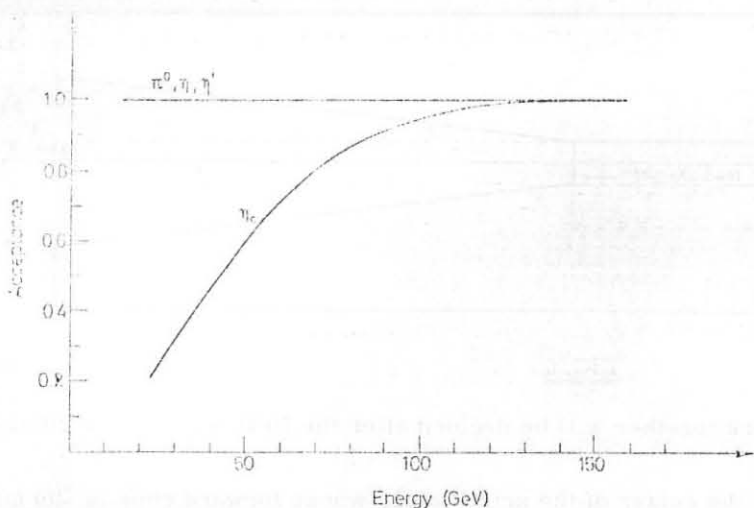


FIG. 8

The total cross section for η_c production is given in Fig. 9 (from ref. 43) assuming $\Gamma_{\gamma\gamma} = 20$ KeV.

We expect that the experimental mass of coherent events will show the η_c peak superimposed over a continuous background due to non resonant vector meson production.

At $3.1 \text{ GeV}/c^2$ it is present the J/ψ peak.

The continuous is characterized by $1/M^2$ behaviour and in η_c region we expect a signal-to-noise ratio of the order of 1, under the assumption that the diffractive photoproduction cross section is 5% of the total photoproduction cross-section.

The J/ψ peak is ~ 20 times larger than η_c one, the identification may be obtained by the ± 40 MeV resolution in mass; a clearer separation will be achieved if the G parity is different.

In this case it is possible to subdivide the events in samples of odd and even number of prongs.

The η_c detector has been developed in order to assure a very high efficiency for coherent production and work at trigger level.

The incoherent events are characterized by a large number of evaporation prongs.

The range of nuclear excitation energy, in the hundreds GeV region, was evaluated by emulsion data at 300 GeV.

The found value was 200 ± 300 MeV for heavy nucleus. Fig. 10 shows the results of MONTE CARLO calculation for $A=165$.

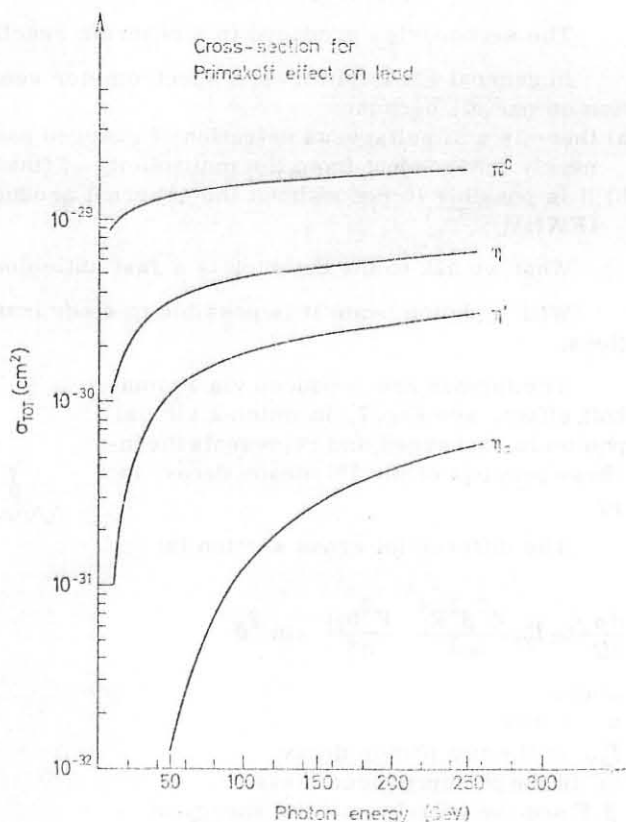


FIG. 9

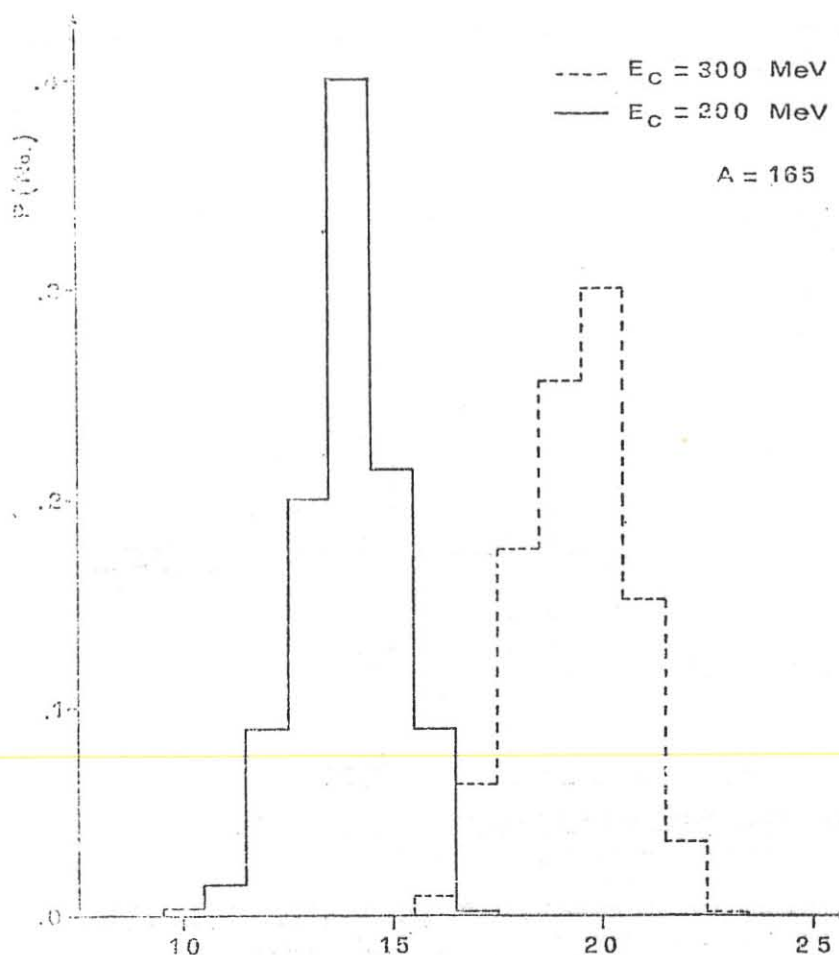


FIG. 10 - No. of neutrons emitted.

With increasing A the neutron emission is enhanced and the lead target for η_c production was chosen because:

- a) it has $Z=82$ and the Primakoff cross section goes as Z^2
- b) when it is excited, it decays by emitting a great number of neutrons and no fission fragment

Suppose ϵ_n is the average efficiency for neutron detection in evaporation region, then the efficiency of the system is:

$$I = (1 - \epsilon_n)^N$$

where N is the average number of neutrons coming from nucleus break-up.

It is reasonable to extract from emulsion data that the incoherent background giving all charged secondaries in the forward cone and only neutrons from nucleus is $\approx 0.003 \sigma_{tot}$ in η_c mass region.

The scintillator dimensions (see Fig. 6) are such that each neutron travels two interaction lengths in the average.

The Milano group developed an electronic chain connected to the PM 8575 faced on each sector⁽⁴⁴⁾.

The revelation threshold for neutron was estimated 30 KeV e. e. and $\epsilon_n \approx 39\%$.

For 14+20 neutrons emitted I is $\approx 9\%_{00} + 5\%_{000}$.

The incoherent background in η_c mass region is so estimated as: $(0.2) + (0.8 \times 10^{-2}) \mu\text{barns}$.

As consequence the incoherent background may be neglected in spite of the big difference in production rate.

2. 3. 2. - Metallic targets.

They have been developed for taking data on multihadron production on nuclei and are capable of identifying the coherent events.

The target consists of (see Fig. 11):

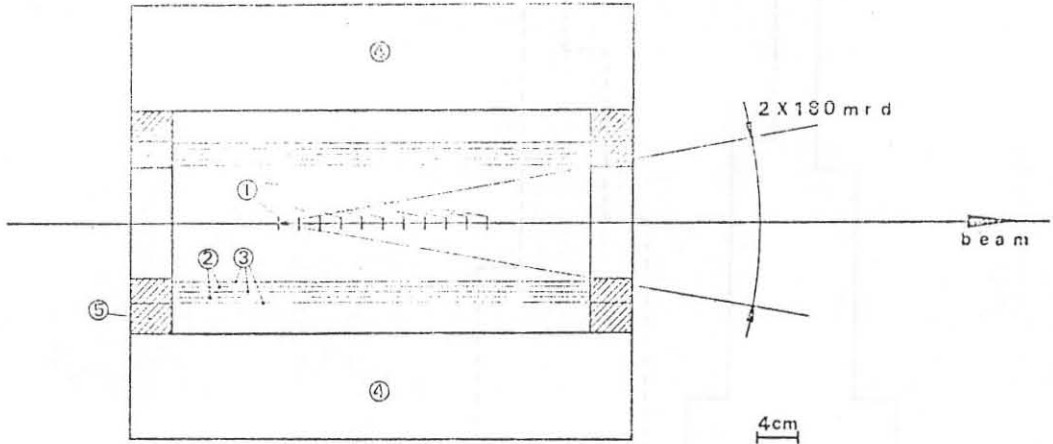


FIG. 11 - Cylindrical MWPC and scintillator: 1) targets; 2) signal wires; 3) h. t. wires; 4) scintillator; 5) frame.

- a) Thin sheets ($\approx 200 \mu\text{m}$) suspended and equally spaced in the central 20 cm along the axis of a cylindrical MWPC. These sheets may range between light and heavy nuclei.
- b) The MWPC has wires parallel to the beam and is supposed to work in proportional regime. The charge division method (c. d. m.) has been introduced for the electronic chain in order to give the coordinate along the wire (expected resolution $\pm 2 \text{ mm}$) and a rough estimation of energy loss.

In such a way it is possible to count charged secondaries between $10^\circ \leq \vartheta \leq 170^\circ$, where the pseudorapidity is a good approximation of the rapidity. The expected pseudorapidity resolution is given in Fig. 12.

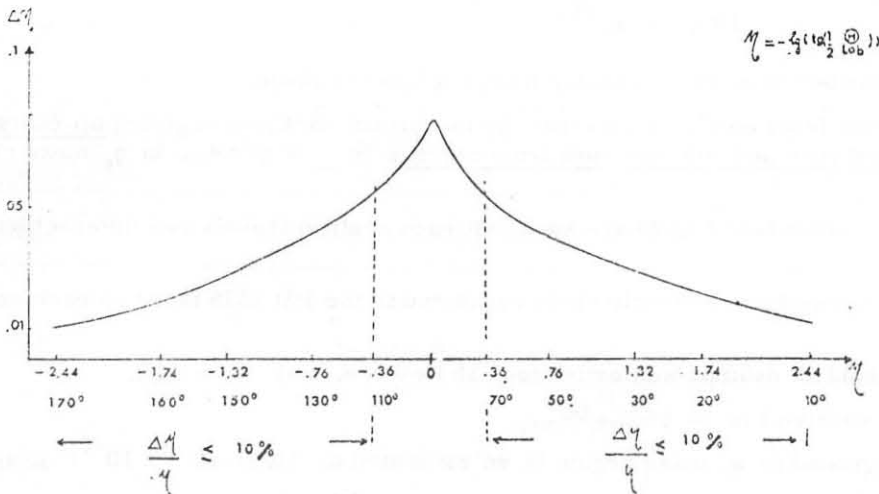


FIG. 12

Another performance is the distinction allowed among fast particles and protons coming from evaporation and quasi direct interaction.

c) A cylindrical scintillator 10 cm thick subdivided in 8 slabs is placed surrounding the chamber. It is studied in the same way as η_c target and gives:

i) A signal of coherent interaction when no charged particles are produced.

The efficiency for tagging the coherent production is $\cong 98+100\%$ ranging from light to heavy nuclei.

ii) It permits to count the number of emitted neutrons, when an incoherent interaction happens in which a low number of charged secondaries or none is spread at big angles.

In conclusion the available data will be:

- a) rapidity (inside the acceptance cone of forward spectrometer) for fast particles, where the pseudorapidity is a bad approximation (for resolution see ref. (41));
- b) pseudorapidity up to 170° in lab. system for any charged particles;
- c) relationships between fast secondaries and particles (neutrons and protons) coming from both evaporation and quasi direct interaction;
- d) selection for coherent production.

With this detector is therefore possible to study in a very detailed way any kind of interaction on nuclei.

In particular what concerns physical questions such as the existence or/and a critical rapidity Y_c (with its dependence from the Atomic number A, the incident energy E and the kind of incoming particle) and the behaviour of projectile and target fragmentation region.

2.3.3. - Helium target.

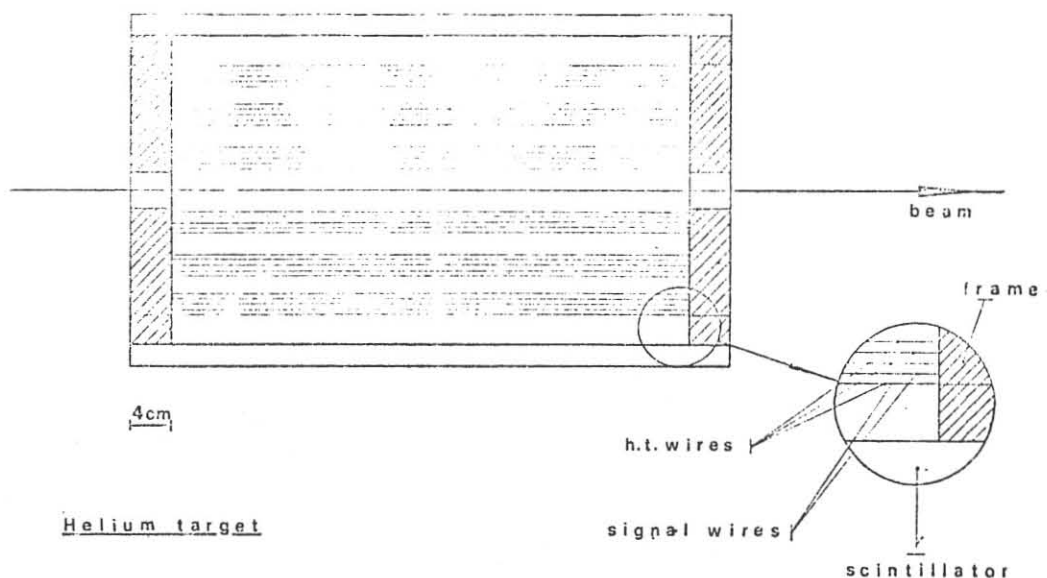
The helium target is a detector capable to study coherent, incoherent, semicoherent and elastic interaction on ${}^4\text{He}$ (45, 46, 47).

In the case of coherent production, it gives the differential cross-section $d\sigma/dt$, through a direct measurement of the recoiling α particle.

It is a gaussees device in which the gas acts simultaneously as target and working medium.

Three cylindrical MWPC's are placed with a diameter of 4, 20, 28 cm respectively and no Mylar walls among them

The c. d. m. is used as in the metallic target.



- (9) L. Bertocchi, Coherent and Inclusive Interactions with Nuclei at High Energy. Gif-sur Yvette, (1975).
- (10) R. J. Glauber, Lectures in Theoretical Physics (edited by E. Britten et al.) (Interscience, 1959) vol. I, pag. 315.
- (11) R. J. Glauber, Proc. 3rd Intern. Conf. on High Energy Physics and Nuclear Structure, New York (1959) (see this paper for a complete set of references on elastic scattering).
- (12) K. S. Kölbig and B. Margolis, Nuclear Phys. B6, 85 (1968).
- (13) C. Bemporad et al., Nuclear Phys. B33, 397 (1971).
- (14) C. Bemporad et al., Nuclear Phys. B44, 627 (1972).
- (15) P. Mühlmann et al., Nuclear Phys. B59, 106 (1973).
- (16) G. Vegni, Phenomenology of diffraction dissociation on Nuclei (Visegrad, 1976).
- (17) B. Gobbi, Proc. Topical Meeting of High Energy Collisions Involving Nuclei, Trieste (1974).
- (18) R. M. Edelstein, Proc. Topical Meeting of High Energy Collisions Involving Nuclei, Trieste (1974).
- (19) G. Bellini et al., Proc. 4th Intern. Symp. on Multiparticles Hadrodynamics, Pavia (1973).
- (20) G. Bellini et al., Proc. 5th Intern. Conf. on High Energy Physics and Nuclear Structure, Uppsala (1973).
- (21) G. Bellini, Proc. Topical Meeting of High Energy Collisions Involving Nuclei, Trieste (1974).
- (22) G. Bellini et al., Phys. Letters 55B, 97 (1975).
- (23) U. E. Kruse et al., Phys. Rev. Letters 32, 1328 (1974).
- (24) J. Pernegr et al., Proc. E. P. S. Conf. Particles Physics, Budapest (1977).
- (25) J. L. Rosen, Proc. 6th Intern. Conf. on High Energy Physics and Nuclear Structure, Santa Fè (1975).
- (26) J. L. Rosen, Proc. Topical Meeting on Multiparticle Production on Nuclei at very High Energy, Trieste (1976).
- (27) G. Fäldt and P. Osland, Nordita preprint (1976).
- (28) K. Gottfried and D. R. Yennie, Phys. Rev. 182, 1595 (1969).
- (29) G. von Bochmann et al., Phys. Letters 33B, 222 (1970).
- (30) G. Fäldt and P. Osland, Nuclear Phys. B87, 445 (1975).
- (31) P. Osland, Proc. 6th Intern. Conf. on High Energy Physics and Nuclear Structure, Santa Fè (1975).
- (32) L. Bertocchi and D. Treleani, Trieste preprint IC/76/31 (1976).
- (33) P. Osland and Treleani, Nuclear Phys. 107B, 493 (1976).
- (34) G. Fäldt, Proc. Topical Meeting on Multiparticle Production on Nuclei at very High Energy, Trieste (1976).
- (35) Proposal to study the coherent 3π , 5π , and $K\pi\pi$ production on nuclei at the SerpuloV Accelerator; PHI/COM-73/32 (1973).
- (36) A. Gurtu et al., Phys. Letters 50B, 391 (1974).
- (37) I. Ötterlund, Proc. Topical Meeting on Multiparticle Production on Nuclei at very High Energy, Trieste (1976).
- (38) C. Halliwell et al., Proc. Topical Meeting on Multiparticle Production on Nuclei at very High Energy, Trieste (1976).
- (39) W. Busza, paper presented at the XVIII Intern. Conf. on High Energy. Tbilisi (1976).
- (40) P. G. Rancoita, invited talk at CERN-Nuclear Physics Series (1976).
- (41) Proposal to the SPS Committee: Comparative Study of Hadron Fragmentation with SPS; CERN/SPSC/74-15, SPSC/P 6 (1974).
- (42) ADDENDUM 2 TO: Comparative Study of Hadron Fragmentation with SPS; CERN/SPSC/74-83, SPSC/P 6 - add. 2 (1974).
- (43) ADDENDUM 3 to Proposal P 6: Status Report on experiment NA1 and Proposal for the determination of (2.8) lifetime via PRIMAKOFF EFFECT CERN/SPSC/76-23/P 6/add. 3 (1976).
- (44) R. Giavina, Preparazione di un'esperienza di produzione multipla da svolgersi all'acceleratore europeo da 400 GeV. Thesis (1977).
- (45) G. Bellini et al., FRAMM internal report, (1975).
- (46) P. G. Rancoita and M. Fiocca, INFN/TC-75/9 (1975).
- (47) P. G. Rancoita, INFN/TC on publication.